# Band shapes in CARS: Background effects and overlapping resonances[a)]

C. M. Roland and W. A. Steele

*Department of Chemistry, The Pennsylvania State University, University Park, Pennsylvania 16802*
(Received 19 November 1979; accepted 27 December 1979)

Quantitative intensity measurements are reported for the CARS spectra of the symmetric stretch ($\nu_3$) mode in liquid $CH_3I$, the totally symmetric stretch ($\nu_1$) in liquid $CCl_4$ and the $Q$ branch for the vibration mode of gaseous $N_2$ at a series of densities. Calculations of the observed band shapes were carried out for both polarized and depolarized bands of $CH_3I$, for the band in $CCl_4$ and for the $N_2$ $Q$ branch at the three lowest densities. Good agreement was obtained after the calculated band shapes were adjusted by varying the values chosen for the nonresonant susceptibility, and for the relaxation times of the vibrational normal coordinates and the reorientation (for the depolarized band). Relaxation times for the liquids and collision broadening factors for the gases are listed; in most cases, the values obtained are more accurate than the corresponding numbers from spontaneous Raman spectra. The problems involved in calculating CARS intensities in the presence of nonresonant susceptibility and overlapping resonances are discussed.

## I. INTRODUCTION

Although theory[1,2] indicates that the generation of coherent antistokes Raman spectra (CARS) is governed by the same resonances in the optical susceptibility that give rise to ordinary spontaneous Raman, there are several features in the detailed expressions for the intensities of the two spectroscopies that give rise to significant differences in the dependence of intensity on frequency, especially when one has overlapping bands or significant background intensity. This paper is devoted to a study of some of these effects. Parts of the vibrational CARS spectrum were measured for three systems: the polarized and depolarized bands for the symmetric stretch of liquid $CH_3I$ at 526 $cm^{-1}$, which has an appreciable hot band intensity overlapping the fundamental; the polarized band for the symmetric breathing mode of liquid $CCl_4$ at ~ 456 $cm^{-1}$ which is an isotopically split band with overlapping combination bands; and the partially resolved polarized $Q$ branch of gaseous $N_2$ at a series of densities. In the first two cases, the spectral widths are considerably larger than the linewidths of the lasers used to generate the signal, which enables one to use a simplified version of the theory in which instrumental sources of broadening are included in an approximate way. The $Q$ branch studies cover a density regime in which the intrinsic width of a spectral line goes from considerably smaller than the laser widths at low density to values at high density that are large enough to cause the spectrum to merge into an unresolved band of width much larger than the laser widths. (Only the low density spectra were analyzed theoretically in this paper.)

Data were obtained using a relatively conventional "three-color" arrangement in which a pump laser with fixed frequency $\omega_1$ and a frequency-scanned Stokes laser at $\omega_2$ are focussed together into the sample, thus generating a CARS beam with frequency $\omega_{as} = 2\omega_1 - \omega_2$. When $\omega = \omega_1 - \omega_2$ equals a Raman frequency $\omega_k$, a resonance in the optical susceptibility causes a striking enhancement in the intensity of the CARS beam. In the present experiments, the $\omega_k$ are vibrational frequencies. However, the resonances are not infinitely sharp, primarily because interactions between the vibrating molecule and its neighbors interrupt the simple harmonic oscillation by producing both dephasing within a single quantum state and transitions between vibrational quantum states. The rotational wings observed in depolarized Raman vibration–rotation spectra also contribute to the CARS spectra. However, in the polarized bands of $CCl_4$ and $CH_3I$ studied here, these wings are weak compared to the central line arising from transitions with $\Delta J = 0$ (where $J$ is the rotational quantum number).

The time-correlation function formalism leads to an expression for the frequency dependence of the vibration–rotation CARS signal $I_{CARS}(\omega)$ which is valid whether or not the rotational wings are significant.[3] We write this expression as

$$I_{CARS}(\omega) = G\left| N\sum_k (\delta f)_k \int_0^\infty C_k(t)\, e^{-i\Delta_k t}\, dt + iB^* \right|^2, \qquad (1)$$

where $\Delta_k = \omega - \omega_k$ and the sum runs over all vibrational transitions that contribute to the observed CARS band. For fundamental vibrational transitions, terms in the sum are generated when transitions due to molecules in thermally excited vibrational states are significant; a sum over all the split fundamentals is also needed when the molecules are not isotopically pure. In Eq. (1), $B^*$ is proportional to the electronic background susceptibility, while $G$, related to the frequency of the incident radiation and energy-momentum conservation, is a slowly varying factor which can be taken as constant over the range of a vibrational spectrum. $C_k(t)$ is the appropriate time correlation function for the $k$th resonance of transition frequency $\omega_k$. Note the CARS intensity is related to the number density difference $N(\delta f)_k$, between the two levels involved in the CARS process.[2] When only one resonance contributes to the sum in Eq. (1), and $\omega_k \gg kT$ so that $\delta f_k \approx 1$, then, in the absence of appreciable electronic background, the CARS intensity distribution is essentially the square of the corresponding spontaneous Raman spectrum.

[a)]This work supported by research grants and a Departmental Instrumentation grant from the National Science Foundation.

 0021-9606/80/245924-09$01.00 

The polarized Raman spectral band shapes for these vibration–rotation transitions are given by a similar time-correlation function formalism:[4]

$$I_{\text{Raman}}(\omega) \propto N \sum_k f_k \int_0^\infty C_k(t) \cos(\Delta_k t)\, dt. \tag{2}$$

Of course, the fact that the various contributions to the Raman are additive makes it easy to separate them and thus to determine $C_k(t)$ by Fourier transform of the appropriate $I_{\text{Raman}}(\omega)$. Numerous studies of the $C_k(t)$ have been reported for simple liquids and in particular for the modes of $CH_3I$[5–9] and $CCl_4$[10,11] studied in this work. Vibrational relaxation functions are currently the object of much theoretical interest[12] because they contain information concerning the mechanisms for vibrational relaxation. For the $CCl_4$ and $CH_3I$ fundamental transitions studied in this work, the spontaneous Raman studies show that the $C_k(t)$ can be taken to be simple exponential decays (with decay constants that are a measure of the vibrational dephasing time); we will also take them to be independent of $k$, which should be quite accurate for isotopic splittings but somewhat less so for a hot band compared to the fundamental. Thus,

$$C_k(t) = \exp(-t/\tau). \tag{3}$$

In the absence of rotational relaxation, one then finds

$$I_{\text{CARS}}(\omega) \propto \left| N \sum_k (\delta f_k) \left( \frac{\tau^{-1} + i\Delta_k}{\tau^{-2} + \Delta_k^2} \right) + iB^* \right|^2. \tag{4}$$

The real part of the electronic susceptibility is associated with two-photon absorption. Since the frequencies of the lasers used in this work lie far from any electronic transition, it is possible to take $iB^*$ to be pure imaginary and constant over the range of the measured spectral bands. Since the CARS intensity is related to the square of the sum in Eq. (1), the nonresonant electronic susceptibility produces cross terms with the resonant part. As a result, not only does the proportionality between the observed CARS intensities and the square of the number density of the resonating molecules break down, but the line shapes and heights are much more complicated than one would calculate for a series of nonoverlapping Lorentzian Raman bands.

It is the purpose of this paper to describe experiments which display the effects of overlap of vibrational transitions and interference between the vibrational resonances and the electronic background, and to attempt a quantitative interpretation of the measured spectra.

## II. EXPERIMENTAL

A schematic diagram of the apparatus is given in an accompanying paper.[13] One of the dye lasers used to excite the CARS spectra was constructed at Penn State. It was held at fixed frequency while a second Molectron dye laser was scanned. Both lasers were pumped by a Molectron nitrogen laser producing ~ 0.5 MW pulses. The two visible dye laser beams were made collinear with a dichroic mirror and focused into the sample. Wave vector matching between incident and generated beams means that the generated CARS beam is collinear with the incident beam. Consequently, the signal was passed through a double monochromator for filtering of stray laser light and any superradiance produced by the dye lasers. The monochromator was thus scanned in parallel with the Molectron dye laser. Scans covered the relatively narrow ranges in frequency associated with the wings of the vibrational bands under investigation. After photomultiplier detection, the signal was boxcar averaged and displayed on a chart recorder.

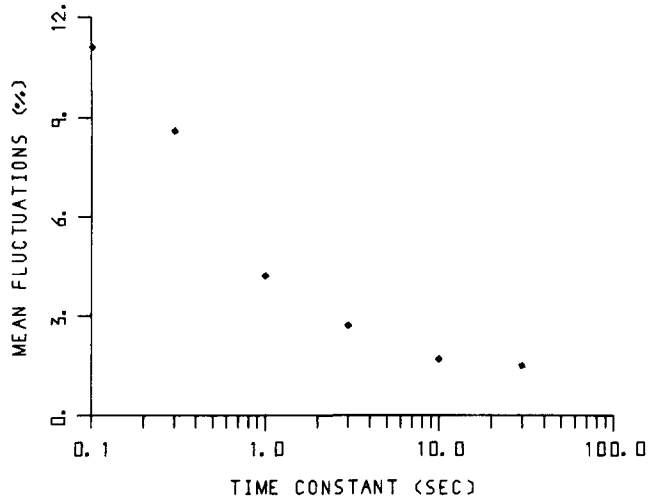


FIG. 1. The root mean square fluctuation in the average CARS signal obtained in the boxcar integrator from a sequence of laser pulses is plotted as a function of the time interval over which data are acquired. Since the laser pulse rate is 10 shots/sec, a time constant of 3 sec corresponds to an average over 30 shots. The value of the fluctuation at a time constant of 0.1 sec primarily reflects the effect of shot-to-shot fluctuations in laser power and pulse shape upon the CARS signal.

One problem that must be solved in any attempt at quantitative intensity CARS measurements is the variations in signal from shot to shot of the input lasers. These variations arise from changes in input laser radiation which are magnified by the nonlinear response of the system, and from changes in the spatial and temporal overlap of the focused radiation in the sample. The degree of overlap is highly sensitive to fluctuations in refractive index and thus can be quite important for liquid samples. Consequently, the averaging of the generated signal was first done using a variable number of laser pulses in order to determine the dependence of the fluctuating average upon the number of pulses. Figure 1 shows this dependence for a typical case. Slowly varying fluctuations in signal were also observed, but we believe these to be due to refractive index variations in the sample which can be due to local fluctuations in temperature. From a number of plots such as that shown in Fig. 1, it was concluded that averaging of ~30 shots was sufficient for the liquids to give intensities that had precisions of a few percent; essentially the same number of shots was needed in the gas phase studies because the improvement due to absence of refractive index fluctuations merely compensated for the weaker signal from the dilute medium.

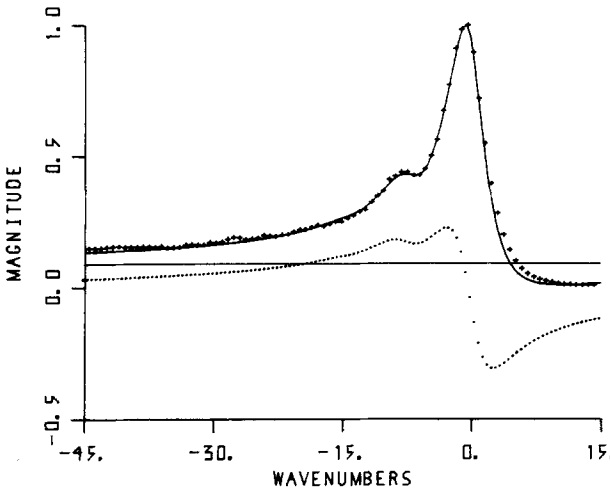


FIG. 2. The experimental polarized CARS spectrum of the $\nu_3$ band of liquid $CH_3I$ is shown by the crosses and the fitted theoretical spectrum, by the solid curve. The relative value of the square of the nonresonant susceptibility is shown by the horizontal line and the cross term between the resonant and nonresonant parts by the dotted line. Experimental spectra in this and other figures have been normalized to give unit intensity at the peak. The zero of the frequency scale is chosen to correspond to the maximum in the spontaneous Raman spectrum. In general, the peak in CARS does not occur at the same frequency as the peak in the spontaneous Raman; in this spectrum, for example, the CARS peak occurs at a frequency shift 0.5 $cm^{-1}$ smaller than the spontaneous Raman value.

### A. Methyl iodide

The polarized CARS spectrum of the $\nu_3$ vibration in methyl iodide is shown in Fig. 2. The prominent shoulder on the low frequency side of the main peak is a hot band, shifted due to anharmonicity. This C–I stretching motion has a frequency of 526 $cm^{-1}$; consequently, at room temperature about 13% of the molecules are in the $v=1$ vibrational level. As expected from its linear dependence on number density [Eq. (2)], the spontaneous Raman hot band intensity directly reflects this population.[8] In the CARS spectrum, however, the maximum of the hot band has ~ 44% of the intensity of the main $v=0$ peak. This anomalously high intensity results from the fact that the peak in the susceptibility for the hot band lies on the imaginary wing of that for the main band. The combination of this imaginary susceptibility with the nonresonant background produces an intensity enhancement. It is generally true that the enhancement will occur on the low frequency side of a resonance, along with a reduction of intensity on the high frequency side, since $B^*>0$ as defined in Eq. (1). Figure 2 also shows a calculated band shape obtained from

$$I_{\mathrm{CARS}}(\omega)=\left|\sum_{v=0}^{4}(v+1)(N_v-N_{v+1})\int_0^\infty e^{-t/\tau_p}\times e^{i(\omega-\omega_v)t}\,dt+iB^*\right|^2, \tag{5}$$

where hot bands up to $v=4$ were included (the contribution from $v=2$ is certainly appreciable);

$$N_v=\exp[-(v+1/2)h\omega_v/kT] \tag{6}$$

and

$$\omega_v=2\pi c\,[526-v(7.2)]\,(\mathrm{sec}^{-1}). \tag{7}$$

The second term in Eq. (7) represents the shift of the hot band frequency due to anharmonicity. The "best-fit" value of the vibrational relaxation time was $\tau_p=1.9\pm0.1$ psec. This correlation time would give a spontaneous Raman band with a HWHM = 2.8 $cm^{-1}$. Bartoli and Litovitz[6] have measured a HWHM = 2.6 $cm^{-1}$ for the Raman band; other workers have found slightly narrower widths.[5,7,8] To obtain these Raman values, the spectrometer resolution must be deconvoluted from the spectrum. In CARS the instrumental resolution is limited by the laser half-widths, which are ~ 0.15 ± 0.05 $cm^{-1}$ in our experiments. In fact, if both the lasers and the experimental lines are approximately Lorentzian, one can subtract[14] the sum of the laser widths from the value of 2.8 $cm^{-1}$ to obtain an estimate of the spontaneous Raman band width of $2.5\pm0.1$ $cm^{-1}$, in reasonable agreement with the directly measured values.

In order to show the relative importance of the background and the cross term, both of these contributions to the total spectral intensity are shown in Fig. 2. It is evident that the constant background contribution is small but nonnegligible, whereas inclusion of the cross term is quite significant, primarily because of its variation with frequency.

In addition to the polarized spectrum, a depolarized CARS spectrum was obtained for $\nu_3$ of liquid $CH_3I$ by setting the planes of polarization of the pump and the Stokes laser at a 90° angle. This spectrum is shown in Fig. 3, together with a curve calculated from Eq.

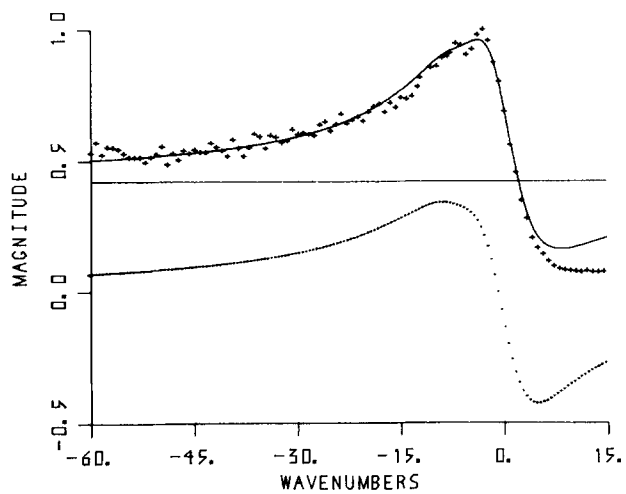


FIG. 3. Depolarized CARS spectrum for the same vibration–rotation band as in Fig. 2. Notation for the curves is also the same as in Fig. 2. This spectrum is obviously less sharply peaked than the polarized band, just as in the spontaneous Raman. (In both cases, the purely vibrational peak is absent from the depolarized spectrum.) The shift of the CARS peak relative to the spontaneous peak is here −3.5 $cm^{-1}$. (This does not mean that the vibrational resonances in the CARS and the Raman susceptibility occur at different frequencies, but that the background and overlap terms in the CARS intensity combine to distort the spectrum so that the CARS peak no longer coincides with the point of maximum resonant susceptibility.)

TABLE I. Electronic susceptibility for liquid $CH_3I$.

| | Polarized | Depolarized |
|---|---|---|
| $B^*$ (sec) | $5.3\times10^{-13}$ | $9.7\times10^{-13}$ |
| $N\,(d\sigma/d\Omega)$ ($cm^{-1}$) | $2.6\times10^{-7}$ | $9.9\times10^{-8}$ |
| $2\,c^4/\hbar\omega_2^4$ (at 580 nm) | $1.38\times10^{7}$ $cm^8$/erg sec | |
| $\chi_{nr}$ ($cm^3$/erg) (at 580 nm) | $1.9\times10^{-12}$ | $1.3\times10^{-12}$ |

(7) using a depolarized relaxation time of $1.0\pm0.1$ psec and best-fit background and cross-term contributions that are also shown in the figure. This spectrum is comparable with the depolarized spontaneous Raman band for $\nu_3$, which lacks a $Q$ branch (i.e., a pure vibrational component). The depolarized Raman band is much broader than the corresponding polarized Raman band because its width is obtained by Fourier transforming the product of the vibrational and the rotational time-correlation functions (if vibration–rotation coupling is neglected). Analysis of the spontaneous Raman band shapes and other experimental studies of molecular rotation in this liquid leads to the conclusion that the relevant orientational time correlation function is nearly exponential with a decay time of $1.6\pm0.2$ psec.[15] If we assume that all shapes are Lorentzian, the experimental depolarized time is given by the reciprocal of the sum of the contributions due to reorientation, vibrational relaxation, and "instrumental" width. Thus,

$$\tau_d = \left(\frac{1}{1.6}+\frac{1}{2.0}+\frac{2}{35}\right)^{-1} \tag{8}$$

$$= 0.85\pm0.2 \text{ psec.}$$

This predicted time agrees well with the value chosen to fit the CARS spectrum. Note that corrections for laser width are less important for the broader depolarized band than for the polarized. It should be emphasized that good fits to the depolarized CARS spectrum could be obtained for a wide range of $\tau_d$ and $B^*$ values, so that the uncertainty in both of these parameters is quite large—at least ± 50%. Numerical results obtained in this study are summarized in Table I. Values of the imaginary part of the electronic background susceptibility used to fit the data are listed in Table I; these were obtained by substituting the known spontaneous Raman cross sections $(d\sigma/d\Omega)$ into the equation[2]

$$\chi_{nr} = \frac{2Nc^4}{\hbar\,\omega_2^4}\left(\frac{d\sigma}{d\Omega}\right)B^*, \tag{9}$$

where $B^{*2}$ is equal to $B^2$ times the maximum CARS intensity. Values of $B^2$ chosen to fit the experiments on $CH_3I$ are shown in Figs. 2 and 3. Finally, we note that our values of $\Delta_k$ are not quite the same as the maxima observed in the CARS intensities because the cross term involving the nonresonant susceptibility changes sign at $\Delta_k$.

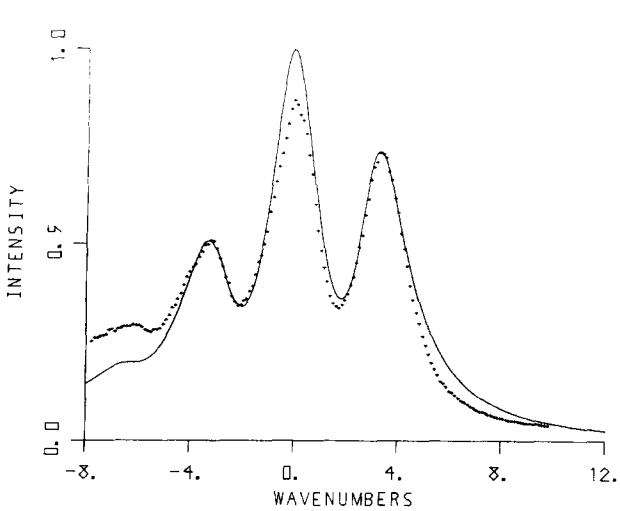


FIG. 4. The experimental CARS spectrum for the $\nu_1$ of pure liquid $CCl_4$ is shown by the crosses. The three peaks are due to the three major isotopic species and the solid curve shows a calculated spectrum. The intensity due to $B^2$ is neglibible on this scale. $B$ is the (imaginary) nonresonant susceptibility.

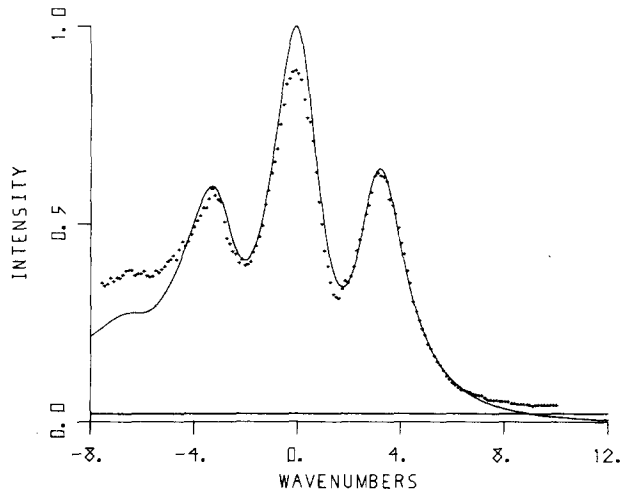


FIG. 5. The same band as shown in Fig. 4, but for a solution which is 67% $CCl_4$ by volume in acetone. The main difference in the two is that the nonresonant background is larger here relative to the resonant signal than in Fig. 4. The horizontal line indicates the intensity due to $B^2$.

## B. Carbon tetrachloride

Polarized CARS spectra for the $(A_{1g})\nu_1$ mode of carbon tetrachloride are given in Figs. 4–6. The isotopic splitting of the spontaneous Raman band gives rise to the three peaks observed in the CARS spectra. These are due to the three most probable isotopic species, which are $C^{35}Cl_4$ (mole fraction = 0.33), $C^{35}Cl_3{}^{37}Cl$ (mole fraction = 0.42), and $C^{35}Cl_2{}^{37}Cl_2$ (mole fraction = 0.21). The experiments on this system were undertaken primarily to illustrate how changes in the relative background susceptibility can affect the isotopic peak intensities. Thus, solutions with varying concentrations of $CCl_4$ in acetone gave the spectra shown in Figs. 5 and 6. The cross term between the resonant term and the background is the product of $B^*$ and the sine transform of the vibrational correlation function. This correlation function was taken to be $\exp(-t/\tau)$, with a single relaxation time regardless of isotopic species. However, regardless of the detailed

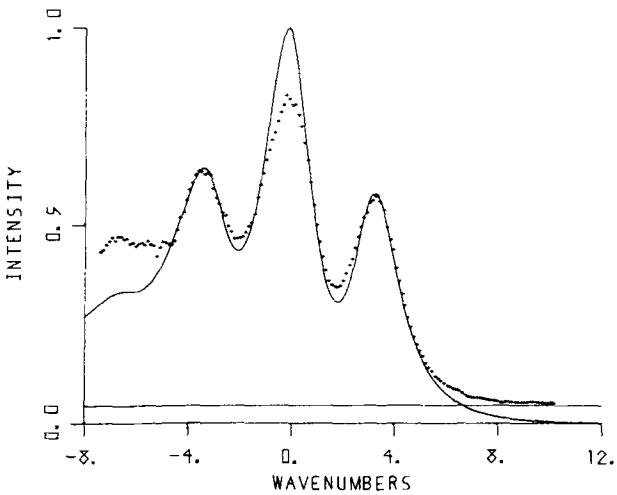


FIG. 6. The same band shown in Figs. 4 and 5 is plotted here for a solution which is 50% $CCl_4$ by volume in acetone. Note that this level of dilution does not appear to affect the appearance of the peaks. In fact, all parameters in the calculated curves were taken to be essentially the same in Figs. 4, 5, and 6 except for the relative magnitude of the nonresonant part of the susceptibility. The contribution of the nonresonant background indicated by the horizontal line is noticeably greater than in Figs. 5 or 4, as one would expect.

nature of this decay, the resulting cross term in the intensity changes sign as the frequency is scanned past the value for the most intense peak (which has been taken to be zero wave number in Figs. 4–6. The actual Raman shift of $\nu_1$ is 458.4 $cm^{-1}$ for the most abundant isotopic species). Since dilution of the $CCl_4$ enhances the relative magnitude of the background, the intensity of all peaks at lower frequencies than zero should increase, which is clearly evident in the figures. Indeed, at 50% dilution by volume with acetone, the less abundant $C^{35}Cl_2{}^{37}Cl_2$ species actually produces a more intense peak than that from $C^{35}Cl_4$. The magnitude of $B^{*2}$ is indicated on the figures, except for pure $CCl_4$, where $B^{*2}$ is too small to be seen on the scale of the figure. Just as in the case of the $CH_3I$ spectra, the cross terms are much more important than the pure background contributions to these spectra.

Also shown in the figures are theoretical spectra fitted to the observed results in the following way: A value of $\tau = 4.5$ psec was chosen to fit the linewidths of all the peaks. For each system, a value of $B^*$ was selected which gave relative heights for the peaks at 3.05 $cm^{-1}$ and at $-3.05$ $cm^{-1}$ ($\pm$ 0.05 $cm^{-1}$) which agreed with the experimentally observed ratio. The spectra were then calculated as a function of frequency. The resulting curves shown in Figs. 4–6 are evidently not in perfect agreement with the experiment. In addition to contributions due to the less abundant isotopic species, the spontaneous Raman spectra[10,11] show that the $\nu_1$ band is flanked by a pair of weak difference bands at about 447 and 474 $cm^{-1}$ (i.e., at frequencies shifted by $-11$ and $+16$ $cm^{-1}$ relative to the zeros in Figs. 4–6). Since we have not attempted to allow for these bands in the calculated CARS spectrum, one should not be too surprised to find deviations from the experimental curves. However, the figure indicates that most of the intensity observed at shifts less than $-6$ $cm^{-1}$ is not due to the fundamental band. It seems likely that the excess intensity at negative shifts is due to the combination band at 447 $cm^{-1}$. Note that the sign of the cross term between the resonance and the background will give positive contributions to the intensity at negative frequency shifts, but negative contributions on the other side of the zero. Thus, one can readily account for the observed asymmetry in the wings of the CARS band.

Measurements of the liquid phase spontaneous Raman polarized $\nu_1$ band indicate a Lorentzian half-width of 1.2 $cm^{-1}$, with an instrumental broadening of 0.5 $cm^{-1}$. This yields an estimated vibrational relaxation time of 7.6 psec, with an uncertainty of roughly 3 psec. When our value of 4.5 psec is corrected for the instrumental broadening due to finite laser linewidth, the CARS experiment yields 6.0 $\pm$ 0.8 psec. We believe that this value of vibrational relaxation time is certainly more precise than that obtained from the spontaneous Raman; we believe that it is also more accurate, primarily because the spectral resolution is considerably higher in the CARS study. Another interesting consequence of the high resolution capability is that the isotopic splittings could be determined to high accuracy ($\pm$ 0.05 $cm^{-1}$), together with the shifts of the peaks with changes in concentration. In particular, it was observed that the peaks shifted by $+0.25$ $cm^{-1}$ and 0.40 $cm^{-1}$ in going from pure $CCl_4$ to the 67% and 50% solutions, respectively.

### C. Nitrogen

Polarized CARS measurements of the partially resolved $Q$ branch of nitrogen gas at a number of densities are shown in Figs. 7–10. Of course, a $Q$ branch

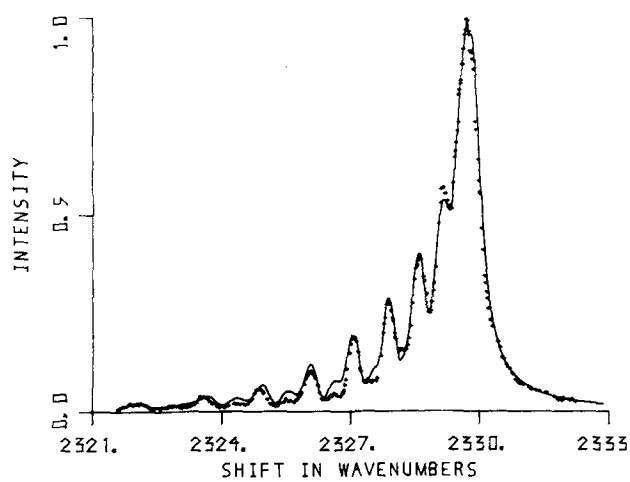


FIG. 7. The crosses show the experimental CARS measurements of the $Q$ branch of the vibrational spectrum of $N_2$ at 1 atm pressure and the smooth curve shows a calculated spectrum. In this case, essentially no fitting parameters were available, since the intensities are obtainable from the spontaneous Raman expressions for $Q$ branch lines and the intrinsic widths of the lines is negligible compared to the known laser line widths. (As noted in the text, some of the parameters of the calculations were "fine tuned"; ie., adjustments within experimental uncertainty were required to give the best fit between the calculated and the measured spectra.)

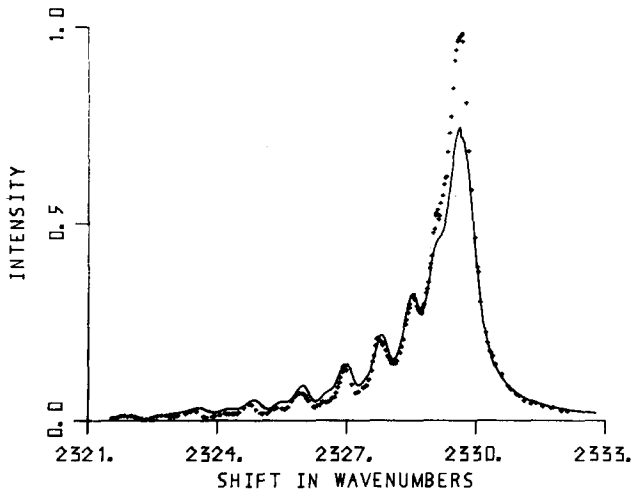


FIG. 8. The crosses show the experimental CARS $Q$ branch of $N_2$ at a density of 2.5 amagat($\simeq$ 40 psia) and room temperature. The solid curve is a calculated spectrum fitted to the experiment using the same parameters ($Q$ branch splitting, intensity ratio, and laser linewidths) as in Fig. 7, except that the collision-broadened intrinsic width of the $Q$ branch lines was adjusted to give the best fit to the spectrum at large $J$ (i.e., in the region 2325–2329 $cm^{-1}$).

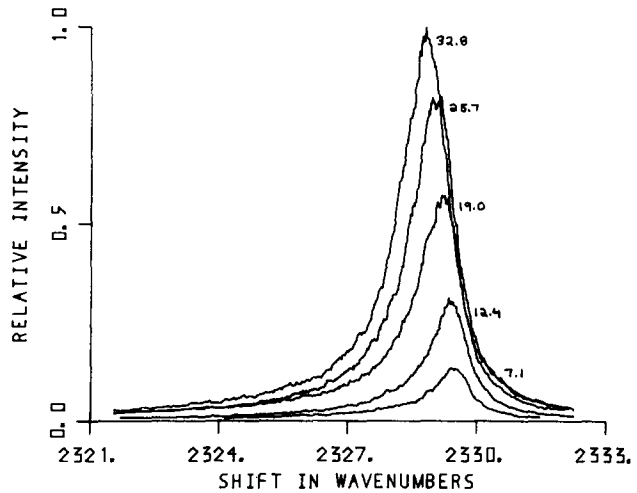


FIG. 10. Experimental measurements of the unresolved CARS $Q$ branch spectra of $N_2$ at several values of the density (indicated next to the appropriate curve, in amagat units). The intensity of the curve for the highest density was normalized to unity at the peak; other intensities are plotted relative to that value. The rapid increase in intensity is primarily a consequence of the dependence of CARS intensity upon the square of the density.

at low density consists in a series of vibrational lines ($\Delta J = 0$, $\Delta v = 1$) separated in frequency due to the change in rotational energy with vibrational state. When intermolecular forces are unimportant, the transition frequencies in the $Q$ branch are given by

$$\omega(J) = \omega_{vib} - \alpha_e J(J+1), \tag{10}$$

where $\omega_{vib}$ is the vibrational frequency and the coupling constant $\alpha_e$ is a measure of the change in moment of inertia (and thus in rotational energy) with vibrational state. We here take $\alpha_e = 0.0178$ $cm^{-1}$ for $N_2$, compared to a literature value of 0.0173 $cm^{-1}$.[17]

As the density of the gas is increased, intermolecular interactions will perturb both the vibrational and the rotational state of a molecule. The frequency and width of the vibrational transition will change, primarily as a result of the isotropic part of the interaction plus a contribution due to coupled vibrational motions.[16] In addition, the rotational energy levels are broadened due to the anisotropic intermolecular potential.[18] Consequently, the broadening of the individual $Q$ branch lines is a result of perturbations to *both* the vibrational and rotational states. However, the broadening is collisional and thus will be proportional to density at low to moderate densities. A successful determination of the linewidths will allow one to extract a cross section for the overall process. The CARS spectra shown in Figs. 7 and 8 show that this will be difficult even at low density. If narrow-line laser sources such as those used by others[19,20] were available for our study, measurements at densities less than 1 amagat would show sufficiently high resolution to simplify the calculation of collision cross section. However, Fig. 8 shows that the intrinsic broadening begins to give appreciable overlap of neighboring lines even at 2 amagat.

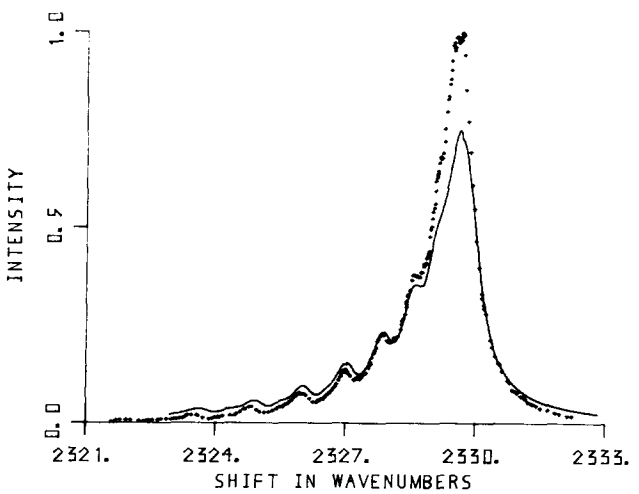


FIG. 9. Same curves as in Fig. 8, but measured at a density of 4.0 amagat.

When the lines in the $Q$ branch are partially overlapped, the situation is complicated. The broadening due to anisotropic forces is a function of the degree of spectral overlap; this in turn depends on which rotational states are involved. A CARS resonance extends further from the line center than the corresponding Raman signal due to the imaginary part of the susceptibility. Greater overlapping of neighboring susceptibilities results (although destructive interference may result in less intensity overlap). This overlapping will amplify the anomalies in the line broadening.

As the density is increased further, the inverse of the collision time approaches the frequency spread of the lines. For complete overlapping, collisions no longer give rise to rotational broadening. The $Q$-branch bandwidth thus remains essentially constant with density

until the collision frequency becomes so high that the molecules pass through many rotational states during one Raman scattering process. When this occurs an "average" frequency is radiated, and hence the bandwidth is seen to decrease with density. Figure 10 indicates that we have not reached the collision narrowing regime (for the CARS $Q$ branch) at the highest density studied.

We have carried out computations of the intensities of these spectra for only the three lowest densities. In these systems, one must treat quantitatively the effects of laser linewidth, which is essentially a Gaussian distribution of frequencies with half-width of $\sim 0.13$ cm$^{-1}$. (The Lorentzian approximation used previously is a simplification that is valid only when the measured line widths are considerably larger than those of the lasers.) Since the nonresonant background susceptibility can be neglected in the low density gases, we will attempt to calculate these $Q$-branch spectra from[13, 14]

$$I_{\mathrm{CARS}}(\omega) \propto \left| \sum_J \mathcal{J}(J) \int_0^\infty e^{-a^2 t^2 - i(\omega - \omega_J)t}\, dt \right|^2, \tag{11}$$

where $\omega_J$ is calculated from Eq. (10). The intensity factor $\mathcal{J}(J)$ is given by[21]

$$\mathcal{J}(J) = \left(16.2 + \frac{J(J+1)}{(2J-1)(2J+3)}\right) \sigma_J (2J+1) \exp\left(\frac{-E(J)}{kT}\right). \tag{12}$$

$E(J)$ is the energy of the $J$th rotational state:

$$E(J) = J(J+1)B_0 - J^2(J+1)^2 D_0, \tag{13}$$

where the rotational constant $B_0$ and centrifugal stretching constant $D_0$ have the values[17]

$$B_0 = 1.9896 \text{ cm}^{-1}, \quad D_0 = 5.76 \times 10^{-6} \text{ cm}^{-1}$$

and $\sigma_J$ is the nuclear spin weight. The value of 16.2 for the trace scattering is determined from the value of the depolarization ratio (0.055 for natural light),[22] and the constant $a$ is a measure of the frequency spread of the laser light.[13] Note that the weak peaks for odd $J$ values are not resolved in any of the experimental spectra even though they can be seen at high $J$ in the calculated $Q$ branches for the two lowest densities. The peak at 2327 cm$^{-1}$ is $Q(12)$; toward the center of the spectrum, $Q(6)$ is resolved only at the lowest density and none of the lines for smaller $J$ can be resolved at all. At the lowest density, the resolution is limited by the laser linewidths and one can say only that the intrinsic widths of the $Q$ branch transitions is less than a few hundredths of a wave number. The effect of collision broadening on these $Q$ branch lines at higher densities was included by inserting a factor $\exp(-t/\tau)$ in the time integral of Eq. (11); this is equivalent to assuming Lorentzian lines in the spontaneous Raman with half-widths $= (2\pi c\tau)^{-1}$ (cm$^{-1}$). Fits to the experimental spectra at high $J$ are shown in Figs. 8 and 9. Values used for the Lorentzian half-widths were $0.07 \pm 0.02$ cm$^{-1}$ at 2.5 amagat and $0.14 \pm 0.02$ cm$^{-1}$ at 4.0 amagat. (Since this width should be proportional to density in this range, one can extrapolate to a value of $0.03 \pm 0.02$ cm$^{-1}$ at 1 amagat, which is negligible compared to the instrumental widths, consistent with the results shown in Fig. 7). The lack of agreement between the low-$J$ parts of the calculated and the experimental spectra in Figs. 8 and 9 is not unexpected. In this region, there is considerable overlap of the $Q$ branch lines even after laser broadening is taken out; theoretical studies of Raman and infrared line shapes under such circumstances show that the calculation of intensity becomes quite complex,[23] and thus one has no reason to believe that the simple formulation used here will adequately describe the CARS experiment.

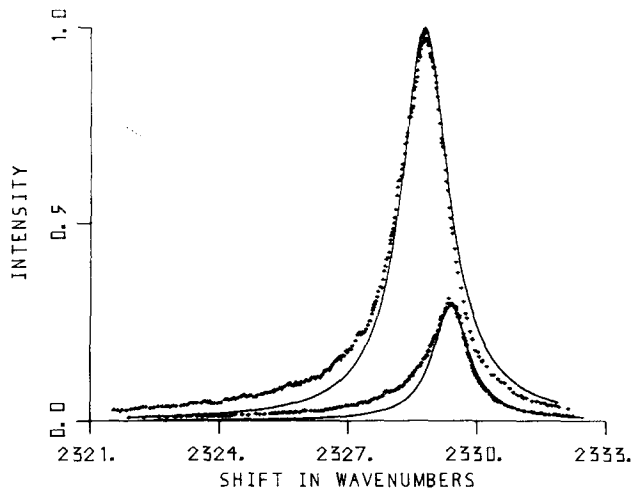


FIG. 11. A comparison between two of the experimental $Q$ branch bands of Fig. 10 and fitted Lorentzian band shapes. The data are shown by crosses and the smooth curves show the Lorentzians for the highest (32.8 amagat) and a low (12.4 amagat) density. Evidently, the Lorentzians cannot give a perfect fit, especially since these experimental curves are still asymmetric relative to the central frequency at $\sim 2329$ cm$^{-1}$ (in the limit of low density, the Q branch lies entirely on the low frequency side of the pure vibrational peak corresponding to $J = 0$).

At even higher densities, all the structure due to individual peaks in the $Q$ branch is lost, as is evident in the spectra shown in Fig. 10. We have not attempted an analysis of the band shapes for these systems; however, it has been suggested[24,25] that the integrated intensity of an isolated CARS band may be used to measure the concentration of the illuminated molecules. In particular, if the band is Lorentzian with half-width $\Delta$, one finds that the integrated intensity should be proportional to $N^2/\Delta$, where $N$ is the density. The bands shown in Fig. 10 are only approximately Lorentzian, as is illustrated in Fig. 11. Nevertheless, values of the integrated intensity are plotted versus $N^2/\Delta$ in Fig. 12. It is evident that the relationship is not linear in this range of density. The likely explanations for this behavior include increasingly large effect of nonresonant background at high density or collision-induced alterations in the Raman susceptibility, as well as experimental artifacts such as systematic changes in the overlap volume of the laser pulses in the medium with increasing density or deviations from the assumed Lorentzian shape. (An analysis based on the assumption of Gaussian shapes gave no better results, either for the fit to the observed spectra or for the variation in integrated intensity.)

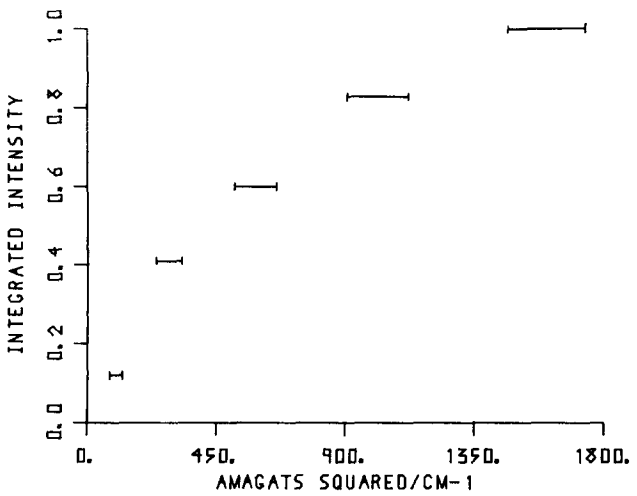


FIG. 12. A plot of the integrated intensity of the CARS $Q$ branch spectra for $N_2$ as a function of the density squared over the bandwidth. If these bands are Lorentzian and if there are no extraneous sources of intensity, the points should fall on a straight line passing through the origin. Even when reasonable estimates of the uncertainty in the band width are included, the experimental results do not conform to this prediction.

We note that Fig. 10 shows a shift in the position of the peak CARS intensity with increasing density. The shift is linear in density, with a slope $d\nu/d\rho = -0.022 \pm 0.002$ cm$^{-1}$/amagat, where $\nu$ is the $N_2$ vibrational frequency. This value is considerably smaller than the shift of $-0.006$ cm$^{-1}$/amagat obtained by Wang and Wright[26] from spontaneous Raman spectra taken at higher density. However, their frequencies extrapolate to a value of 2328.2 cm$^{-1}$ at $\rho = 0$ which is noticeably lower than the value of 2329.9 cm$^{-1}$ obtained by others.[17,27] Since the unresolved $Q$ branch exhibits a maximum at a frequency lower than the vibrational frequency, it is possible that the small slope of Wang and Wright is the resultant of a small positive shift due to a decrease in $Q$ band width and a larger negative shift of the vibrational frequency.

## III. CONCLUSIONS

We have analyzed a number of CARS spectra generated by systems which display interference effects, due either to nonresonant susceptibility or to overlapping resonances or both. In some cases, it was necessary to carefully treat the effects of finite linewidth in the lasers used to generate the signals. The agreement obtained between calculated and experimental spectra was satisfactory. Although the spectral resolution in this work is only moderately good by CARS standards, it is comparable with that obtained in the best spontaneous Raman experiments. Consequently, linewidth parameters obtained for these liquids (and particularly for $CCl_4$) are often more accurate than those reported previously.

In addition to the spontaneous Raman studies,[10,11] vibrational relaxation in the $\nu_1$ mode has been directly measured in liquid $CCl_4$ using picosecond pulse techniques.[28] A dephasing time of $7.0 \pm 0.8$ psec and an isotopic splitting of $2.9 \pm 0.15$ cm$^{-1}$ were reported, in good agreement with our values.

Since the coherent nature of the nonlinear process that generates a CARS signal means that the spectral intensity results from first summing and then squaring the contributions to the optical susceptibility, one finds that relatively small terms in the sum can be quite important because of the cross terms in the square. As a result, CARS can be a useful technique for the study of weak effects. As a case in point, the hot band in the $CH_3I$ CARS spectrum is considerably enhanced relative to the spontaneous Raman; this obviously facilitates studies of the shape and position of the hot band as a function of density or solvent. Our analysis indicates that quantitative information can be obtained from such CARS spectra.

It does appear that a better theoretical framework is needed, especially for the $Q$ branch at high densities where spectral overlap of individual rotational lines is extensive (but incomplete); similar problems undoubtedly will arise when lines in the $O$ and $S$ branches are similarly overlapping. However, this is a difficult problem in any spectroscopy and should not prevent the successful interpretation of CARS intensities obtained for the vibration–rotation bands of simple molecules in the liquid or in the gas at low density.

[1]H. C. Andersen and B. S. Hudson, in *Molecular Spectroscopy* Vol. 5, (Specialist Periodical Reports (Chemical Society, London, 1977).
[2]J. W. Nibler, W. M. Shaub, J. R. McDonald, and A. B. Harvey, in *Vibrational Spectra and Structure*, Vol. 6, edited by J. Durig (Elsevier, Amsterdam, 1978).
[3]J. O. Bjarnason, B. S. Hudson and H. C. Andersen, J. Chem. Phys. **70**, 4130 (1979).
[4]R. G. Gordon, Adv. Magn. Reson. **3**, 1 (1968).
[5]H. S. Goldberg and P. S. Pershan, J. Chem. Phys. **58**, 3816 (1973).
[6]F. J. Bartoli and T. A. Litovitz, J. Chem. Phys. **56**, 404 (1972).
[7]J. H. Campbell, J. F. Fisher, and J. Jonas, J. Chem. Phys. **61**, 346 (1974).
[8]R. B. Wright, M. Schwartz, and C. H. Wang, J. Chem. Phys. **58**, 5125 (1973).
[9]P. van Konynenberg and W. A. Steele, J. Chem. Phys. **56**, 4776 (1972).
[10]J. T. Kenney and F. X. Powell, J. Chem. Phys. **47**, 3220 (1967).
[11]S. Sunder and R. E. D. McClung, Chem. Phys. **2**, 467 (1973).
[12]D. Oxtoby, Adv. Chem. Phys. **40**, 1 (1979).
[13]C. M. Roland and W. A. Steele, J. Chem. Phys. **73**, 5919 (1980), preceeding article.
[14]W. A. Yuratich, Mol. Phys. **38**, 625 (1979).
[15]W. A. Steele, Adv. Chem. Phys. **34**, 1 (1976).
[16]A. D. May, G. Vargese, J. C. Stryland, and H. L. Welsh, Can. J. Phys. **42**, 1058 (1964).
[17]J. Bendtsen, J. Raman Spectrosc. **2**, 133 (1974).
[18]C. G. Gray and J. van Kranendonk, Can. J. Phys. **44**, 2411 (1966).
[19]J. P. E. Taran, in *Tunable Lasers and Applications*, edited by A. Mooradian, T. Jeeger, and P. Stokseth (Springer, New York, 1975), p. 378.
[20]W. Nitsch and W. Kiefer, Opt. Commun. **23**, 240 (1977).
[21]G. Placzek, in *Handluch der Radiologie*, edited by E. Marx

(Akademische Verlagsgesellschaft, Leipzig, 1939), Vol. VI, Part 2, p. 209.
[22]T. Yoshino and H. J. Bernstein, J. Mol. Spectrosc. **2**, 213 (1958).
[23]For example, see D. E. Fitz and R. A. Marcus, J. Chem. Phys. **59**, 4380 (1973) and references contained therein. Also, papers dealing directly with the Raman line broadening problem include: J. Fiutak and J. van Kranendonk, Can. J. Phys. **40**, 1085 (1952); *ibid*. **41**, 21 (1963); J. van Kranendonk, Can. J. Phys. **41**, 433 (1963); C. G. Gray and J. van Kranendonk, Can. J. Phys. **44**, 2411 (1966).
[24]W. M. Tolles and R. D. Turner, Appl. Spectrosc. **31**, 96 (1977).
[25]W. B. Roh and P. W. Schreiber, Appl. Opt. **17**, 1418 (1978).
[26]C. H. Wang and R. B. Wright, J. Chem. Phys. **59**, 1706 (1973).
[27]W. Nitsch and W. Kiefer, Opt. Commun. **23**, 240 (1977).
[28]A. Laubereau, G. Wochner and W. Kaiser, Opt. Commun. **17**, 91 (1976); Phys. Rev. A **13**, 2212 (1976).